Submitted to the 9th IFAC International Symposium on Advances in Automotive Control, Orléans, France, 24-27 June 2019

Air-management and fueling strategy for diesel engines from multi-layer control perspective

Adrian Ilka, **Nikolce Murgovski**, **Jonas Fredriksson** and **Jonas Sjöberg**

Department of Electrical Engineering, Chalmers University of Technology, Hörsalsvägen 9-11, SE-412 96, Gothenburg, Sweden. E-mail: adrian.ilka@chalmers.se

Abstract: The paper proposes a novel control design procedure for air management and fueling strategy (AMFS) of diesel engines in lights of a multi-layer control structure (MLCS). Furthermore, novel sufficient stability conditions in the form of linear matrix inequalities are derived (using slack variables to reduce the conservativeness) for grid-based linear parameter-varying systems. The gain-scheduled controller for AMFS is designed to track a reference torque trajectory requested by higher control layers from MLCS, with the objective of minimizing diesel consumption and pollutants' emissions. For controller design a reduced order grid-based linear parameter-varying model is obtained from the detailed benchmark model published by Eriksson et al. (2016). The controller is validated on the benchmark model using the road profile Söderälje-Norrköping.

Keywords: Multi-layer control; optimal control; robust control; linear parameter-varying systems; diesel engine; air-path system.

1. INTRODUCTION AND PRELIMINARIES

Transport is one of the key components in economic growth and globalization, and also the largest drainer of energy, especially oil. In a typical economy, up to 25% of all energy consumption accounts for transportation purposes. The main source of energy is obtained from oil, so transport can also be accounted as the largest drainer of the limited oil reserves. In fact, about 60% of all the global oil consumption is attributed to transport activities (Rodrigue et al., 2017). In addition, transport is a significant contributor to global warming (through emission of carbon dioxide CO_2) and to air pollution (including nitrous oxides NO_x and particulates) (Fuglestvedt et al., 2008). In the EU, transport industry contributed to about 21% of the total CO_2 emissions in 2017, 72.9% of which is from road transport (EEA, 2017).

Therefore, reducing energy consumption and minimizing emissions of vehicles is of utmost importance nowadays. One approach is to improve the vehicle design, by e.g. reducing the aerodynamic drag and rolling resistance, or by developing novel powertrain concepts, such as those in hybrid-electric, fuel-cell-electric or fully electric vehicles. Another approach is to improve the software solutions, by e.g. intelligently controlling the available actuators in the various powertrain concepts, see e.g. NASEM (2015) and references therein. One effective way to address this problem from an optimal control perspective is to use the so-called *multi-layer control structure*.

⋆ This work has been financed in part by the Swedish Energy Agency (P43322-1), and by IMPERIUM (H2020 GV-06-2015).

1.1 Multi-layer control structure (MLCS)

The optimal control problem for improving powertrain efficiency has the objective of minimizing fossil fuel consumption and pollutants' emissions, while taking the advantage of the novel technologies that provide predictive and dynamic information on traffic and road topography and enable communication between vehicles and infrastructure. Due to the emerging control complexity, the typical approach for obtaining a computationally tractable solution is splitting the original optimal control problem into finite number of subproblems, organized into several control layers, see Fig. 1.

The first control layer from the top is the *Transport mission management* (MM), which is a layer that runs a model predictive control (MPC) algorithm in the cloud, or possibly in the vehicle, in order to generate reference targets for the layer below. The aim of the MM is to minimize fuel consumption, wear and discomfort for the entire mission, or up to hundreds of kilometers, subject to electric charge sustaining and traffic information, and bounds on speed, battery energy and travel time. For more info see Hamednia et al. (2018). The next two layers are the *Energy buffers management* (EM), and the *Gear and powertrain mode management* (PM). These on-board layers are minimizing fuel consumption, wear and discomfort for a look-ahead horizon of up to 10 km. The EM optimizes vehicle velocity and battery state of charge using sequential convex programming while the PM layer optimizes gear and engine on/off state trajectories using dynamic programming. For more info the readers are refereed to Johannesson et al. (2015); Murgovski et al.

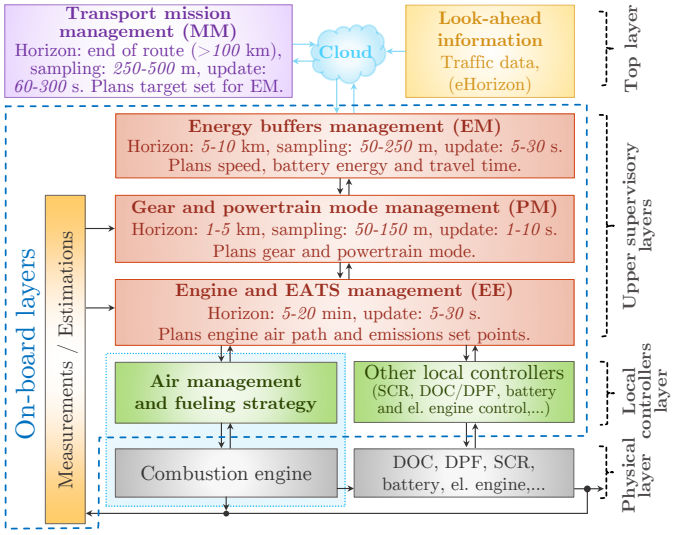

Fig. 1. Multi-layer control structure.

(2016); Hovgard et al. (2018). The next on-board layer is the *Engine and Exhaust After-Treatment System (EATS) management* (EE), which uses an economic nonlinear MPC based strategy. The objectives of this layer are to improve the fuel economy while fulfilling real-driving emissions within work-based-windows (introduced in the Euro VI emission legislation for heavy-duty vehicles). For more info see Feru et al. (2016); Karim et al. (2018). The above three layers (EM, PM and EE) are generating reference trajectories and set points for the controllers in the local controllers layer.

1.2 Air management and fueling strategy (AMFS)

One of the important sub-problems within the local controllers layer is the air management and fueling strategy of the combustion engine. In this paper we consider a diesel engine with variable geometry turbine (VGT) and exhaust gas recirculation (EGR), as illustrated in Fig. 2.

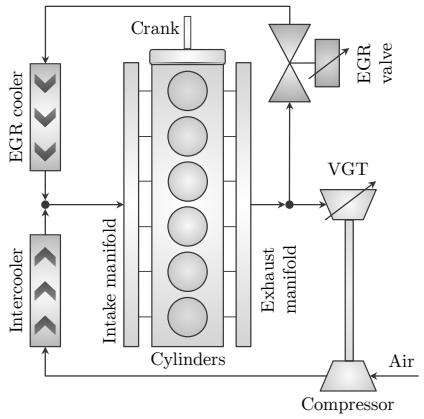

Fig. 2. Air path system of diesel engine. The engine includes an exhaust gas recirculation (EGR) and a variable geometry turbine (VGT).

Many approaches exist in literature for controlling such engines, whilst among the most prominent are the gain-scheduled and/or the linear parameter-varying (LPV) control techniques (Wei and del Re, 2007; Wei et al., 2008; Liu et al., 2008; Alfieri et al., 2009; Hong et al., 2015; Buenaventura et al., 2015; Hong et al., 2017; Park et al., 2017). So far in general, the local controllers for VGT and EGR are designed to follow prescribed set-points for intake manifold pressure, air mass flow and/or air fraction. However, considering the interface within the multi-layer control structure described above, we can conclude that a new low-level controller is needed, where the upper layers are relived of the fast dynamics (intake/exhaust manifold pressures, turbine speed etc.).

The rest of the paper is organized into four sections. The introduction and preliminaries is followed by prescribing the new control structure and algorithm in Section 2. The LPV modeling and controller design is described in Section 3, proceeded with simulation experiments in Section 4. Finally, Section 5 closes the paper with some concluding remarks. The mathematical notation of the paper is as follows. Given a symmetric matrix $P = P^T \in \mathbb{R}^{n\times n}$, the inequality $P \succ 0$ ($P \succeq 0$) denotes the positive definiteness (semi definiteness) of the matrix. Matrices, if not explicitly stated, are assumed to have compatible dimensions.

2. CONTROL STRUCTURE FOR AMFS

Considering the multi-layer control structure (Section 1.1), the following objectives could be selected for the local controller for AMFS:

1) Follow the reference torque, while
2) minimizing the fuel consumption, and
3) fulfilling the constraints (on inputs, states and outputs).

The EGR control is not considered as part of the AMFS, since for the studied system EGR is controlled by the EATS controller, which carries the main responsibility of limiting NO_x emissions. The air path system of diesel engine with VGT can be represented in a polytopic LPV form,

$$\begin{aligned} \dot{x}(t) &= A(\theta(t))x(t) + B(\theta(t))u(t), \\ z(t) &= C_z(\theta(t))x(t) + D_z(\theta(t))u(t), \\ y(t) &= Cx(t), \end{aligned} \tag{1}$$

where $x(t) \in \mathbb{R}^{n_x} = [p_{im}(t), p_{em}(t), \omega_t(t)]^T$ is the state vector, where $p_{im}(t)$ (Pa) and $p_{em}(t)$ (Pa) are the input and exhaust manifold pressures, and $\omega_t(t)$ (rpm) is the turbine speed; $u(t) \in \mathbb{R}^{n_u} = [u_\delta(t), u_{vgt}(t)]^T$ is the control input vector, where $u_\delta(t)$ (mg/stroke) is the fuel injection, and $u_{vgt}(t)$ (%) is the VGT position; $y(t) \in \mathbb{R}^{n_y} = M_e(t)$ is the measurable output, where $M_e(t)$ (Nm) is the engine torque; and $z(t) \in \mathbb{R}^{n_z} = [W_f(t), 1/\lambda(t)]^T$ is the performance output vector, where $\lambda(t)$ (-) is the air-to-fuel ratio, and $W_f(t)$ (kg/s) is the fuel flow into the cylinders,

$$W_f(t) = n_{cyl} u_\delta(t) n_e(t), \tag{2}$$

where n_{cyl} is a known constant and $n_e(t)$ (rpm) is the engine speed. The matrix functions $A(\theta(t))$, $B(\theta(t))$, $C_z(\theta(t))$, and $D_z(\theta(t))$ belong to a convex set, a polytope with n_{wp} vertices that can be formally defined as

$$\{A(\theta(t)), B(\theta(t)), C_z(\theta(t)), D_z(\theta(t))\} = \sum_{i=1}^{n_{wp}} \{A_i, B_i, C_{z_i}, D_{z_i}\}\,\theta_i(t),\ \sum_{i=1}^{n_{wp}} \theta_i(t) = 1,\ \theta_i(t) \geq 0, \tag{3}$$

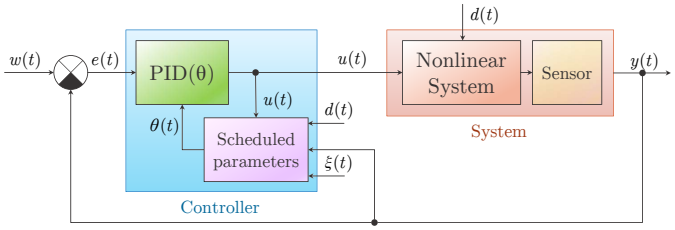

Fig. 3. Closed-loop system with the gain-scheduled PID controller.

where A_i, B_i, C_{z_i}, D_{z_i}, and C are constant matrices of corresponding dimensions, and $\theta_i(t) \in \Omega$, $i = 1, 2, \ldots, n_{wp}$ are constant or time-varying known parameters calculated from the scheduling parameters (engine torque $M_e(t)$, engine speed $n_e(t)$, and VGT position $u_{vgt}(t)$).

We propose a gain-scheduled PID$_f$ controller in the form

$$\begin{aligned} u(t) =& K_P(\theta(t))e(t) + K_I(\theta(t)) \int_0^t e(\tau)d\tau \\ &+ K_D(\theta(t))e_{d_f}(t), \end{aligned} \tag{4}$$

where $e(t) = y(t) - w(t)$, wherein $w(t)$ is the reference signal (in our case the reference torque $M_{e_{ref}}$). Furthermore, $K_P(\theta(t))$, $K_I(\theta(t))$, and $K_D(\theta(t))$ are the proportional, integral, and derivative gains belonging to a convex set similar to (3), and $e_{D_f}(t)$ is derivative error filtered by

$$G_f(s) = \frac{c_f s}{s + c_f}, \tag{5}$$

where c_f is a filtering coefficient. The closed-loop system structure can be sketched as shown in Fig. 3, where $d(t)$ is the disturbance input (in our case the engine speed $n_e(t)$), and $\xi(t)$ is a signal form the supervisor, which can be used to adjust the performance of the controller. Investigation of the benefits from such adjustments has been excluded from the scope of this paper and $\xi(t)$ is not further discussed.

The control law (4) should be designed according to the objectives stated above. One way to do that is to formulate the controller design as an output-feedback linear quadratic regulator (ofLQR) design problem, where the quadratic cost function can be defined as

$$\begin{aligned} J_\infty = \int_0^\infty \Big(& x(t)^T Q(\theta(t))x(t) + u(t)^T R(\theta(t))u(t) \\ & + 2x(t)^T S(\theta(t))u(t) \Big) dt, \end{aligned} \tag{6}$$

where

$$\begin{bmatrix} Q(\theta(t)), & S(\theta(t)) \\ S(\theta(t))^T, & R(\theta(t)) \end{bmatrix} \succeq 0,$$

$$Q(\theta(t)) = Q_x(\theta(t)) + C_z(\theta(t))^T Q_z C_z(\theta(t)),$$

$$R(\theta(t)) = Q_u(\theta(t)) + D_z(\theta(t))^T Q_z D_z(\theta(t)),$$

$$S(\theta(t)) = Q_{xu}(\theta(t)) + C_z(\theta(t))^T Q_z D_z(\theta(t)).$$

The weighting matrices $Q_x(\theta(t)) \in \mathbb{R}^{n_x \times n_x}$, $Q_u(\theta(t)) \in \mathbb{R}^{n_u \times n_u}$, $Q_{xu}(\theta(t)) \in \mathbb{R}^{n_x \times n_u}$, and $Q_z \in \mathbb{R}^{n_z \times n_z}$ can be used to tune the closed-loop system in order to balance the trade-off between the reference tracking, fuel consumption and emissions (particulates), as well as to fulfill the input/output/state constraints.

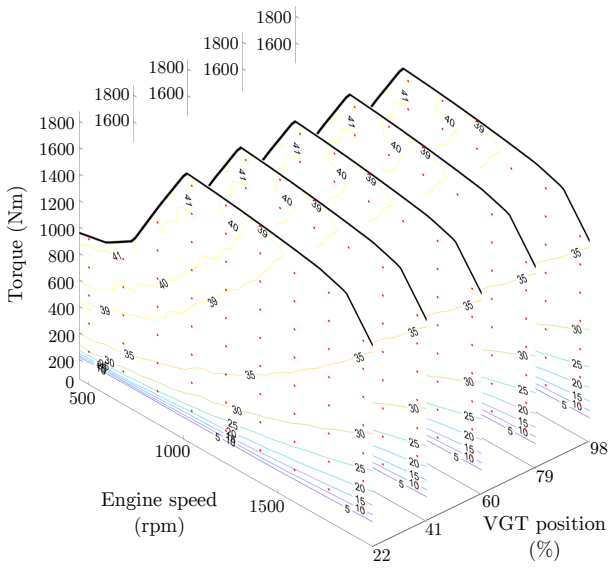

Fig. 4. Grid points used for linearization along the working trajectory generated by the three scheduled parameters (engine torque and speed, and VGT position).

3. LPV MODELING AND CONTROL

This section presents the proposed LPV modeling and control algorithms. First, the LPV modeling and model validation are described, which are followed by the LPV controller design.

3.1 LPV modeling

There are several techniques to obtain linear-parameter varying models. For a comprehensive survey, readers are referred to Toth (2010) and references therein. One of the approaches is the *grid-based* LPV identification and modeling technique, which is also supported by the Control System Toolbox, Matlab (The Mathworks, Inc., 2017). The LPV model in the form of (1) has been obtained by reducing the nine-state benchmark model, published by Eriksson et al. (2016), to the three slowest states, as described in Section 2. The reduced model is then linearized about 330 working (grid) points (Fig. 4) along the trajectory generated by the three scheduling parameters (engine torque $M_e(t) \in [0, 1800]$ Nm, engine speed $n_e(t) \in [400, 2000]$ rpm and VGT position $u_{vgt}(t) \in [20, 100]$ %).

Comparison of the original nine-state benchmark model (Eriksson et al., 2016) with the obtained three-state grid-based LPV model is shown in Fig. 5. Beside the comparison of system states, measured and performance outputs, the absolute percentage errors (APE), mean absolute percentage errors (MAPE) and max absolute percentage errors (maxAPE) are displayed as well. These percentage errors are calculated as:

$$\begin{aligned} \text{APE}_i &= \frac{|S_{o_i} - S_{t_i}|}{\max|S_{o_i}|} 100\%, \; i = 1, 2, \ldots, n, \\ \text{MAPE} &= \frac{1}{n} \sum_{i=1}^{n} (APE_i), \; \text{maxAPE} = \max(APE_i), \end{aligned} \tag{7}$$

where n is the number of samples, and S_{o_i} and S_{t_i} are the i-th original and test samples.

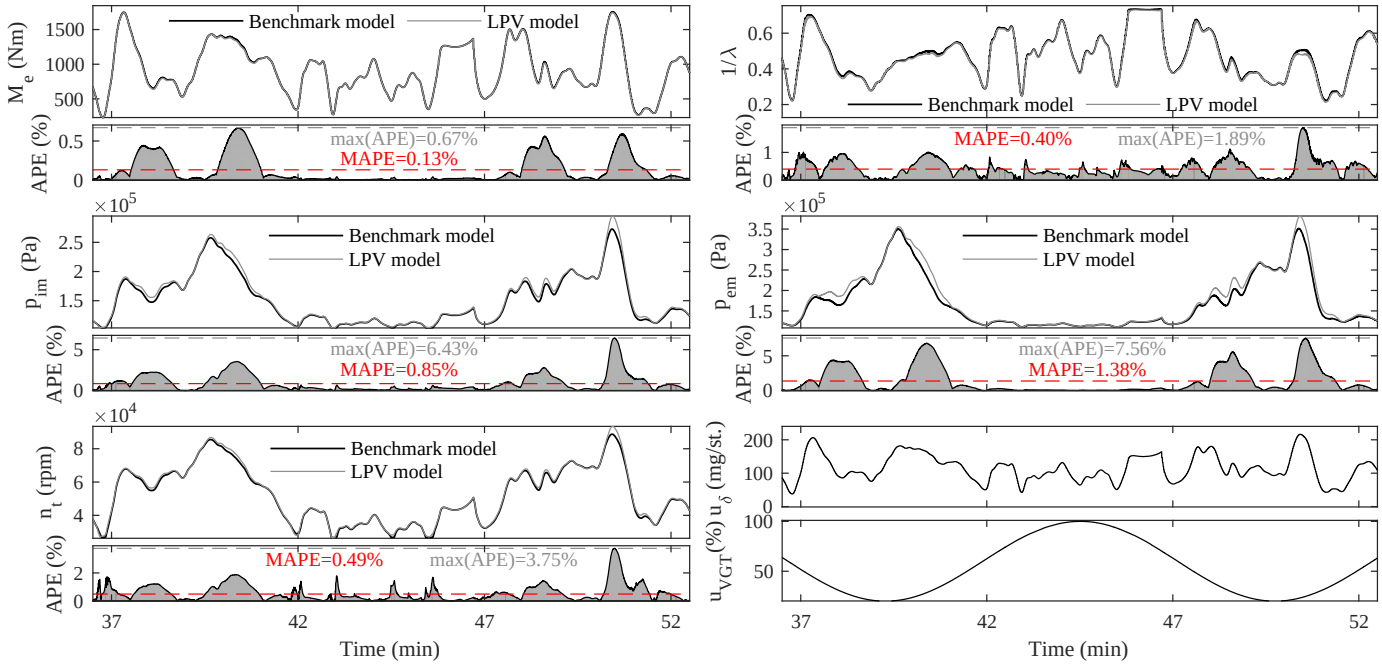

Fig. 5. Comparison of the original benchmark model (Eriksson et al., 2016) with the reduced order grid-based LPV model (16 min slice from the 91 min driving cycle).

3.2 LPV controller design

Most of the LQR-based LPV and/or gain-scheduled output-feedback controller design approaches formulates the controller design problem as an optimization problem subject to constraints in the form of linear/bilinear matrix inequalities (LMIs/BMIs) (Veselý and Ilka, 2013; Ilka and Veselý, 2014; Veselý and Ilka, 2017; Ilka and Veselý, 2017). These optimization problems can be solved efficiently by using LMI and/or BMI solvers for small and medium sized problems. However, big LMI and/or BMI problems with high number of variables (controller gain matrices, Lyapunov matrices, auxiliary matrices etc.) could lead to the problem being unsolvable.

In this paper, we propose a systematic procedure to deal with the high number of variables owing to the 330 grid points, by splitting the whole optimization problem into small sub-optimization problems. Then the results of these sub-optimization problems are united to get the sub-optimal gain-scheduled output-feedback controller. The overall stability is then tested with a novel stability criteria developed for this procedure.

First, the system (1) is augmented with the sensor dynamics, which we considered as a first order filter with time constant $T_f = 0.01$ s (the new output is then the sensor output $y_s(t)$). Then the uncertainty polytopes (with eight vertices) are obtained for each vertex of the system (1), by linear interpolation in the space trajectory created by the scheduled parameters (Fig. 6) with 1/3 distance from the neighbouring working (grid) points. Finally local robust LQR-based PID$_f$ controllers are designed for these uncertainty polytopes using the **`oflqr`** toolbox (Ilka, 2018), with filter coefficient $c_f = 100$, and weighting matrices $Q_x = \mathrm{diag}([0, 0, 0, 10^2, 10^5, 10^3])$, $Q_u = \mathrm{diag}([3 \times 10^{-3}, 1])$, $Q_{xu} = 0$ and $Q_z = \mathrm{diag}([1, 5 \times 10^5])$. The gain-scheduled controller in the form (4) is then constructed from the

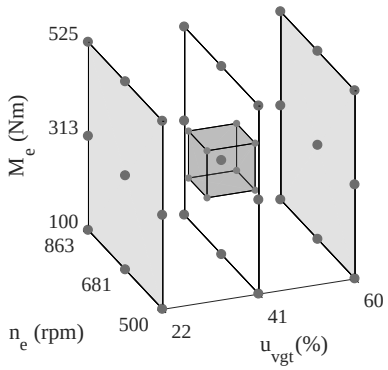

Fig. 6. Uncertainty polytope around the working (grid) point ($M_e = 312.5$ Nm, $n_e = 681$ rpm, $u_{vgt} = 41$ %).

family of these local PID$_f$ controllers. The weighting coefficients in Q_x, related to the PID$_f$ controller (proportional $Q_{x_{4,4}}$, integral $Q_{x_{5,5}}$ and derivative $Q_{x_{6,6}}$) are selected to obtain certain reference tracking performance (0 steady state error, no overshoot, and settling-time less then 0.5 s). The weighting coefficients in Q_z are chosen to balance the trade of between fuel consumption and emissions (particulates, by minimizing $1/\lambda$).

Since the reference signal $w(t)$ (reference engine torque) is bounded, we can simplify the derivation by setting $w(t) = 0$. Then, by augmenting the system (1) with additional state variables such as the integral of the measurable output $y_{s_I}(t) = \int_0^t y_s(\tau)d\tau$, and the filtered derivative output $y_{s_{D_f}}$ using the derivative filter (5), the control law (4) can be transformed to

$$u(t) = F(\theta)\tilde{y}(t) = F(\theta(t))\tilde{C}(\theta(t))\tilde{x}(t), \qquad (8)$$

where $\tilde{y}(t)^T = [y_s(t)^T,\, y_{s_I}(t)^T,\, y_{s_{D_f}}(t)^T]$ is the augmented output vector and $\tilde{x}(t)^T = [x(t)^T,\, y_{s_I}(t)^T,\, y_{s_{D_f}}(t)^T]$ is the

augmented state vector. The augmented system is then

$$\begin{aligned}\dot{\tilde{x}}(t) &= \tilde{A}(\theta(t))\tilde{x}(t) + \tilde{B}(\theta(t))u(t),\\ \tilde{y}(t) &= \tilde{C}\tilde{x}(t),\end{aligned} \tag{9}$$

where

$$\tilde{A}(\theta(t)) = \begin{bmatrix} A(\theta(t)), 0, & 0 \\ C, & 0, & 0 \\ B_f C, & 0, & A_f \end{bmatrix}, \tilde{B}(\theta(t)) = \begin{bmatrix} B(\theta(t)) \\ 0 \\ 0 \end{bmatrix},$$

$$C = \begin{bmatrix} C, & 0, & 0 \\ 0, & I, & 0 \\ B_f C, & 0, & A_f \end{bmatrix}, \; B_f = c_f I, \; A_f = -c_f I.$$

The next Theorem formulates the sufficient stability conditions for the closed-loop system formed by system (9) and control law (8)

$$A_{cl}(\theta(t)) = \tilde{A}(\theta(t)) + \tilde{B}(\theta(t))F(\theta(t))\tilde{C}. \tag{10}$$

Theorem 1. The closed-loop system (10) is quadratically stable for all $\theta \in \Omega$ if there exist a positive definite matrix $P \in \mathbb{R}^{\tilde{n}_x \times \tilde{n}_x}$ and matrices N_j, $j = 1, 2, \ldots, 6$ of corresponding dimensions, such that the following LMIs hold

$$M_i = \begin{bmatrix} M_{i_{11}}, M_{i_{12}}, M_{i_{13}} \\ M_{i_{12}}^T, M_{i_{22}}, M_{i_{23}} \\ M_{i_{13}}^T, M_{i_{23}}^T, M_{i_{33}} \end{bmatrix} \prec 0, \; i = 1, 2, \ldots, n_{wp}, \tag{11}$$

where

$$\begin{aligned}
&M_{i_{11}} = N_1^T + N_1, \;\; M_{i_{12}} = P - N_1^T \tilde{A}_i + N_2 - N_4^T F_i \tilde{C},\\
&M_{i_{13}} = N_3 + N_4^T - N_1^T \tilde{B}_i,\\
&M_{i_{22}} = -N_2^T \tilde{A}_i - \tilde{A}_i^T N_2 - N_5^T F_i \tilde{C} - \tilde{C}^T F_i^T N_5,\\
&M_{i_{23}} = N_5^T - N_2^T \tilde{B}_i - \tilde{A}_i^T N_3 - C^T F_i^T N_6,\\
&M_{i_{33}} = N_6^T + N_6 - N_3^T \tilde{B}_i - \tilde{B}_i^T N_3.
\end{aligned}$$

Proof 1. Consider the Lyapunov function candidate as

$$V(t) = \tilde{x}(t)^T P \tilde{x}(t). \tag{12}$$

The first derivative of the Lyapunov function (12) is then

$$\begin{aligned}\dot{V}(t) &= \dot{\tilde{x}}(t)^T P \tilde{x}(t) + \tilde{x}(t)^T P \dot{\tilde{x}}(t)\\ &= v(t)^T \begin{bmatrix} 0, P, 0 \\ P, 0, 0 \\ 0, 0, 0 \end{bmatrix} v(t),\end{aligned} \tag{13}$$

where $v(t)^T = [\dot{\tilde{x}}(t)^T, \tilde{x}(t)^T, u(t)^T]$. To separate the Lyapunov matrix P from the system's matrices the auxiliary matrices N_j, $j = 1, 2, \ldots, 6$ of corresponding dimensions are used in the following form

$$\begin{aligned}&2(N_1\dot{\tilde{x}}(t) + N_2\tilde{x}(t) + N_3 u(t))^T\\ &\qquad (\dot{\tilde{x}}(t) - \tilde{A}(\theta(t))\tilde{x}(t) - \tilde{B}(\theta(t))u(t)) = 0,\end{aligned} \tag{14}$$

$$\begin{aligned}&2(N_4\dot{\tilde{x}}(t) + N_5\tilde{x}(t) + N_6 u(t))^T\\ &\qquad (u(t) - F(\theta(t))\tilde{C}\tilde{x}(t)) = 0,\end{aligned} \tag{15}$$

Summarizing equations (14) and (15) with the time derivative of the Lyapunov function (13) we can write

$$v(t)^T M(\theta(t)) v(t) \leq -\epsilon v(t)^T v(t), \; \epsilon \geq 0, \tag{16}$$

where

$$\begin{aligned}
&M_{11} = N_1^T + N_1,\\
&M_{12} = P - N_1^T \tilde{A}(\theta(t)) + N_2 - N_4^T F(\theta(t))\tilde{C},\\
&M_{13} = N_3 + N_4^T - N_1^T \tilde{B}(\theta(t)),\\
&M_{22} = -N_2^T \tilde{A}(\theta(t)) - \tilde{A}(\theta(t))^T N_2 - N_5^T F(\theta(t))\tilde{C}\\
&\qquad -\tilde{C}^T F(\theta(t))^T N_5,\\
&M_{23} = N_5^T - N_2^T \tilde{B}(\theta(t)) - \tilde{A}(\theta(t))^T N_3 - C^T F(\theta(t))^T N_6,\\
&M_{33} = N_6^T + N_6 - N_3^T \tilde{B}(\theta(t)) - \tilde{B}(\theta(t))^T N_3,
\end{aligned}$$

Table 1. Reference tracking properties of the closed-loop system.

Attribute	*Value*
Maximal settling-time:	0.3 s
Overshoot:	-
Steady-state error:	-
Reference tracking MAPE:	7.2894×10^{-4} %
Reference tracking max(APE):	0.0589 %

which implies that the closed-loop system is stable for some $\epsilon \geq 0$ if $P \succ 0$.

From inequality (16) for $\epsilon \to 0$ we can obtain

$$M(\theta(t)) \prec 0, \tag{17}$$

where $M(\theta(t))$ is convex in θ, therefore it is enough to check the definiteness at the vertices of θ, i.e. we get the LMIs (11) which completes the proof.

4. SIMULATION EXPERIMENT

To evaluate the obtained gain-scheduled controller the road profile Söderälje-Norrköping and the benchmark model from Eriksson et al. (2016) have been used. For the simulation, the reference torque $M_{e_{ref}}(t)$, engine speed $n_e(t)$ and gears are given by the supervisory layers. Simulation results are given in Fig. 7, where beside the engine torque and speed ($M_e(t)$ and $n_e(t)$), inverse air-to-fuel ratio ($1/\lambda(t)$), turbine speed ($n_t(t)$), VGT position ($u_{vgt}(t)$), fuel injection ($u_\delta(t)$), gear, road slope and altitude are shown as well.

Fig. 8 and Table 1 show that the objectives for reference tracking are fulfilled. The total fuel mass for the whole driving cycle is $M_f = 32.78$ kg with the proposed controller, which is less (up to 3.53 %) compared to total fuel masses obtained with fixed VGT positions fulfilling the constraint on the air-to-fuel ratio. This is illustrated in Fig. 9 as well, with relation to different constraints.

5. CONCLUSION

This paper proposes a novel suboptimal controller and control design algorithm for AMFS of diesel engines, which is designed to track a reference torque trajectory requested by higher control layers. For controller design, a reduced order grid-based LPV model is obtained from the detailed benchmark model published by Eriksson et al. (2016). Finally, a simple sub-optimal gain-scheduled PID$_f$ controller is designed using the **`oflqr`** toolbox (Ilka, 2018) and by a novel stability criteria developed for this procedure. Future research will focus on the extension of the established results for NO_x emissions control of diesel engines with the EGR system, as well as to investigate the possible benefits from using the signal $\xi(t)$ (coming from supervisors) introduced in Section 2.

REFERENCES

Alfieri, E., Amstutz, A., Guzzella, L., 2009. Gain-scheduled model-based feedback control of the air/fuel ratio in diesel engines. Control Engineering Practice 17 (12), 1417–1425.

Buenaventura, F. C., Witrant, E., Talon, V., Dugard, L., 2015. Air fraction and EGR proportion control for dual

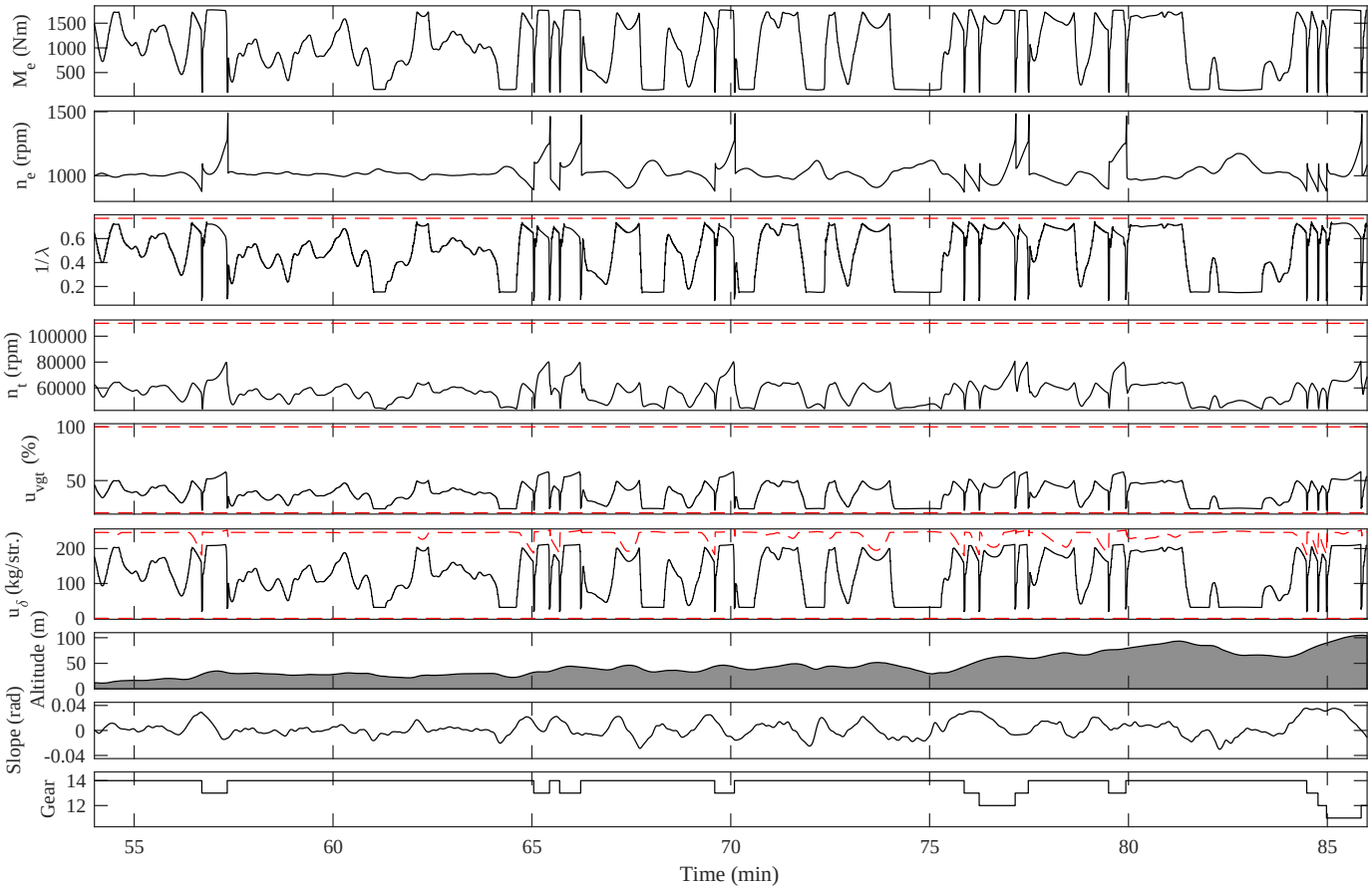

Fig. 7. Simulation results with the proposed controller (32 min slice from the 91 min driving cycle). The road profile Söderälje-Norrköping has been used to evaluate the proposed gain-scheduled controller. The red dashed lines are the constraints to be fulfilled.

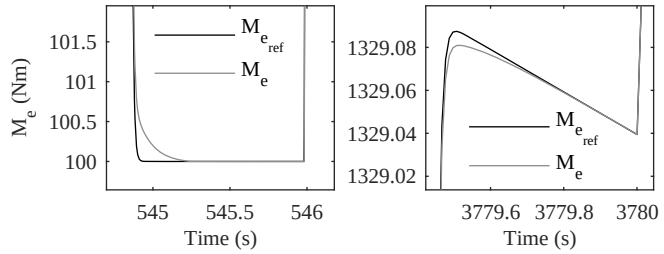

Fig. 8. Zoomed slices from the driving cycle which shows the reference tracking properties of the closed-loop system.

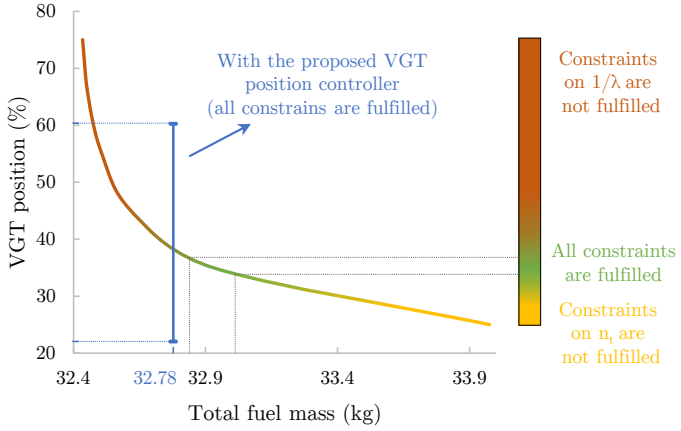

Fig. 9. Fuel consumption for fixed VGT positions and for controlled VGT positions.

loop EGR diesel engines. Ingenieria y Universidad, Pontifica Universidad Javeriana, Faculty of Science 19 (1), 115–133.

EEA, 2017. European union emission inventory report 1990-2015 under the UNECE convention on long-range transboundary air pollution. Tech. rep., European Environment Agency.

Eriksson, L., Larsson, A., Thomasson, A., 2016. The AAC2016 Benchmark - Look-Ahead Control of Heavy Duty Trucks on Open Roads. IFAC-PapersOnLine 49 (11), 121 – 127, 8th IFAC Symposium on Advances in Automotive Control AAC 2016.

Feru, E., Murgovski, N., de Jager, B., Willems, F., 2016. Supervisory control of a heavy-duty diesel engine with an electrified waste heat recovery system. Control Engineering Practice 54, 190 – 201.

Fuglestvedt, J., Berntsen, T., Myhre, G., Rypdal, K., Skeie, R. B., 2008. Climate forcing from the transport sectors. Proceedings of the National Academy of Sciences 105 (2), 454–458.

Hamednia, A., Murgovski, N., Fredriksson, J., 2018. Predictive velocity control in a hilly terrain over a long look-ahead horizon. In: 5th IFAC Conference on Engine and Powertrain Control, Simulation and Modeling (E-CoSM18). pp. 1–6.

Hong, S., Park, I., Chung, J., Sunwoo, M., August 2015. Gain scheduled controller of EGR and VGT systems with a model-based gain scheduling strategy for diesel engines. In: 4th IFAC Workshop on Engine and Powertrain Control, Simulation and Modeling E-COSM. Colombus, Ohio, USA, pp. 1–6.

Hong, S., Park, I., Shin, J., Sunwoo, M., May 2017. Multivariable controller with a gain scheduling strategy for the exhaust gas recirculation and variable geometry turbocharger systems in diesel engines. ASME Journal of Dynamic Systems, Measurement, and Control 139.

Hovgard, M., Jonsson, O., Murgovski, N., Sanfridson, M., Fredriksson, J., 2018. Cooperative energy management of electrified vehicles on hilly roads. Control Engineering Practice 73, 66 – 78.

Ilka, A., 2018. Matlab/Octave toolbox for structurable and robust output-feedback LQR design. IFAC-PapersOnLine 51 (4), 598 – 603, 3rd IFAC Conference on Advances in Proportional-Integral-Derivative Control PID 2018.

Ilka, A., Veselý, V., March-April 2014. Gain-Scheduled Controller Design: Variable Weighting Approach. Journal of Electrical Engineering 65 (2), 116–120.

Ilka, A., Veselý, V., 2017. Robust guaranteed cost output-feedback gain-scheduled controller design. IFAC-PapersOnLine 50 (1), 11355 – 11360, 20th IFAC World Congress.

Johannesson, L., Nilsson, M., Murgovski, N., 2015. Look-ahead vehicle energy management with traffic predictions. IFAC-PapersOnLine 48 (15), 244 – 251, 4th IFAC Workshop on Engine and Powertrain Control, Simulation and Modeling E-COSM 2015.

Karim, M. R., Egardt, B., Murgovski, N., Gelso, E. R., 2018. Supervisory control for real-driving emission compliance of heavy-duty vehicles. In: 5th IFAC Conference on Engine and Powertrain Control, Simulation and Modeling (E-CoSM18). pp. 1–6.

Liu, L., Wei, X., Zhu, T., July 2008. Quasi-LPV gain scheduling control for the air path system of diesel engines. In: Control and Decision Conference, CCDC 2008. pp. 4893–4898.

Murgovski, N., Egardt, B., Nilsson, M., 2016. Cooperative energy management of automated vehicles. Control Engineering Practice 57, 84 – 98.

NASEM, 2015. Review of the 21st Century Truck Partnership: Third Report. National Academies of Sciences, Engineering, and Medicine, The National Academies Press, Washington, DC.

Park, I., Hong, S., Sunwoo, M., 2017. Gain-scheduled EGR control algorithm for light-duty diesel engines with static-gain parameter modeling. International Journal of Automotive Technology 18 (4), 579–587.

Rodrigue, J.-P., Notteboom, T., Comtois, C., Slack, B., 2017. The Geography of Transport Systems, 4th Edition. Routledge, Taylor & Francis Group Ltd.

The Mathworks, Inc., 2017. MATLAB R2017a. The Mathworks, Inc., Natick, Massachusetts.

Toh, K. C., Todd, M., Tütüncü, R. H., 1999. SDPT3 – a MATLAB software package for semidefinite programming. Optimization methods and software 11, 545–581.

Toth, R., 2010. Modeling and Identification of Linear Parameter-Varying Systems, 1st Edition. Vol. 403 of Lecture Notes in Control and Information Sciences. Springer-Verlag Berlin Heidelberg.

Veselý, V., Ilka, A., Sep. 2013. Gain-scheduled PID controller design. Journal of Process Control 23 (8), 1141–1148.

Veselý, V., Ilka, A., July 2017. Generalized robust gain-scheduled PID controller design for affine LPV systems with polytopic uncertainty. Systems and Control Letters 105 (0), 6–13.

Wei, X., del Re, L., May 2007. Gain Scheduled H_∞ Control for Air Path Systems of Diesel Engines Using LPV Techniques. IEEE Transactions on Control Systems Technology 15 (3), 406–415.

Wei, X., del Re, L., Liu, L., 2008. Air path identification of diesel engines by LPV techniques for gain scheduled control. Mathematical and Computer Modelling of Dynamical Systems 14 (6), 495–543.